ANL/MSD/CP-91586

NATIONAL INSTITUTE OF STANDARDS AND TECHNOLOGY – TEXAS INSTRUMENTS INDUSTRIAL COLLABORATORY TESTBED*

M. T. Postek, T. Wheatley, and S. Jones
National Institute of Standards and Technology
Gaithersburg, MD 20899

M. Bennett
Texas Instruments, Inc.
Dallas, TX

N. J. Zaluzec
Materials Science Division
Argonne National Laboratory
Argonne, IL 60439

October 1998

Paper submitted to the Microscopy and Microanalysis held in Atlanta, GA on July 12-16, 1998.

*Work supported in part by the U. S. Department of Energy, BES-Materials Sciences, under Contract W-31-109-ENG-38.

DISCLAIMER

DISCLAIMER

Portions of this document may be illegible in electronic image products. Images are produced from the best available original document.

Xe precipitates at grain boundaries in Al under 1 MeV electron irradiation

Charles W. Allen[1,*], Mingui Song[2], Kazuo Furuya[2], Robert C. Birtcher[1], Kazutaka Mitsuishi[2] and Ulrich Dahmen[3]

[1]Argonne National Laboratory, Argonne, IL 60439 USA
[2]National Research Institute for Metals, Tsukuba, Ibaraki 305-0003, JAPAN
[3]Lawrence Berkeley National Laboratory, Berkeley, CA 94720 USA

*Corresponding Author:
Dr. Charles W. Allen
Materials Science Division—Building 212/E211
Argonne National Laboratory
9700 South Cass Avenue
Argonne, IL 60439 USA
Phone: (630) 252-4157
FAX: (630) 252-4798
E-Mail: allen@aaem.amc.anl.gov

Running Title:
Xe precipitates at grain boundaries in Al

Key Words:
high-resolution electron microscopy, Al, bicrystal, Xe precipitate, grain boundary, irradiation

Total Number of Pages Submitted (including this cover page): 11

Total Number of Figures Submitted: 5

Xe precipitates at grain boundaries in Al under 1 MeV electron irradiation

C. W. Allen[1,*], M. Song[2], K. Furuya[2], R. C. Birtcher[1], K. Mitsuishi[2] and U. Dahmen[3]
[1]Argonne National Laboratory, Argonne, IL 60439 USA, [2]National Research Institute for Metals, Tsukuba, Ibaraki 305-0003, JAPAN and [3]Lawrence Berkeley National Laboratory, Berkeley, CA 94720 USA
*To whom correspondence should be addressed

Abstract Crystalline nanoprecipitates of Xe have been produced by ion implantation into mazed bicrystalline Al at 300 K, in which the matrix grain boundaries are mainly 90 deg tilt boundaries. Within Al grains, Xe nanocrystals are fcc, isotactic with the Al and cuboctohedral in shape with {111} and {100} facets. With an off-axial imaging technique, the nanocrystals were structure imaged against a relatively featureless matrix background. In contrast to metal precipitates in Al, such as Pb, Xe precipitates straddling a matrix grain boundary are bicrystals as small as approximately 2 nm in diameter. Larger Xe precipitates tend to avoid boundaries which are inclined away from asymmetrical orientation and which thus have a significant twist component . Under the 1 MeV electron irradiation employed for HREM observation, small Xe nanocrystals near a grain boundary may migrate to the boundary and coalesce with other Xe precipitates. The structural observations are rationalized on a simple geometrical interpretation.

Keywords high-resolution electron microscopy, Al mazed bicrystal, Xe precipitate, grain boundary, irradiation

Received

Introduction

When a noble gas is implanted into a metal, a fine dispersion of precipitates forms. Below some critical size, these precipitates, typically up to about 10 nanometers in diameter, are close-packed crystals which are isotactic and incommensurate with the host matrix; i.e., the orientation of the precipitate and matrix coincide but the interface is incoherent. In the case of Xe implanted to fluences greater than approximately $2x10^{18}$ m^{-2} at 300 K into Al, the critical quasi-equilibrium size for solid-liquid transition at 300 K is 8–10 nm. As crystalline solids, both Al and Xe form elementary fcc lattices with 4 atoms per unit cell, the Xe being a loosely bound van der Waals solid with a lattice parameter approximately 1.5 times that of Al [1]. The Xe lattice parameter increases slightly with increasing particle size, the Xe evidently obeying its equation of state under the influence of the surface tension of the matrix cavities [2]. Under Frenkel pair producing electron irradiation, Al-Xe alloys are driven far enough from equilibrium that a number of dynamic phenomena involving the Xe precipitates are observed, including melting and crystallization, migration, faulting and coalescence [3–5]. Observed in transmission electron microscopy under high-resolution conditions with respect to the Xe, such phenomena can appear quite spectacular.

The purpose of this paper is to examine the morphologies of a dispersion of Xe precipitates in mazed bicrystalline Al, with particular emphasis on the structure and behavior of the Xe at and near 90° tilt boundaries. The experiments were performed in situ in a high-resolution high-voltage electron microscope in which realtime observations of precipitate behavior were video recorded duringthe electron irradiation.

Materials and methods

Transmission electron microscopy (TEM) specimens were prepared at Lawrence Berkeley National Laboratory by evaporation of high purity Al onto a (100) Si substrate at 550 K. The Si was subsequently mechanically dimpled and ion milled from the Si side to perforation of the Al film. The Al film consisted of a duplex grain structure with $[110]_{Al}$ plane normal parallel to the $[100]_{Si}$ plane normal. Specimens were then implanted at Argonne National Laboratory at 475 K with 35 keV Xe to a dose of $6x10^{18}$ m^{-2}. The mean depth of implanted Xe is 25 nm from Monte Carlo simulation by TRIM 95 [6] for these implantation conditions.

High resolution electron microscopy (HREM) and additional implantation of 50 keV Xe to a dose of $3x10^{19}$ m^{-2} were performed in the JEOL ARM-1000 high voltage electron microscope (HVEM) in the High Resolution Beams Station of the National Research Institute for Metals (NRIM) at Tsukuba, Japan. The HVEM was operated with a LaB_6 electron source at 1 MeV, for which the demonstrated point-to-point image resolution was 0.13 nm and Scherzer defocus was 55 nm [7]. 1 MeV electron irradiations with simultaneous imaging were performed with a nearly focused electron beam, with and without a condenser aperture. It was found that good structure imaging of Xe precipitates could be achieved even with the intense electron beam so that irradiation-induced structural changes could be observed and recorded in real time.

In order to decrease the contrast of the Al matrix relative to that of the Xe precipitates for high resolution imaging, the specimen was tilted approximately 3 degrees off <110> zone axes of the Al bicrystals about a 115 reciprocal lattice vector of one of the matrix orientations, and the objective lens was defocused to a value at which the contrast transfer function for low order Al spacings was near zero. Because of the small size and larger lattice parameter of the Xe crystals, the Xe structure images were not noticeably degraded by this off-axial imaging technique, in agreement with image simulations [8]. Achieving similar contrast in two adjacent grains was nonetheless tedious, however. The high resolution image was video tape recorded continuously (S-VHS) in real time at 30 frames per second with a running five frame average.

Results and discussion

Microstructure of Xe precipitates

Fig. 2 is an overview of a bicrystalline region including a variety of Xe precipitate morphologies and sizes. Facet orientations are indicated for a large precipitate in each of the matrix grains, as are the orientations of symmetrical (S) and asymmetrcal (A) 90 ° tilt boundaries. Traces of these boundaries are also indicated in Fig. 1 in relation to the bicrystal orientations, as described by Dahmen and Westmacott [9]. In Fig. 2 Xe precipitates lacking structural contrast are fluid, including some which are much smaller than the quasi-equilibrium size limit for crystalline Xe in Al at 300 K. It is evident that the precipitates which straddle the matrix grain boundary are themselves also bicrystals.

The energetics of cuboctahedral precipitates within a matrix grain are under consideration by Dahmen [10] with particular reference to Pb in Al. In the absence of lattice strains such as those due to precititate/matrix coherency or to differential thermal expansion effects, excess enthalpy is associated with the {100} and {111} interfaces and interface intersections along edges and at apeces. The difficulty of the problem is compounded further for the case of a precipitate at a matrix grain boundary, as illustrated by the sketches in Fig. 3. Fig. 3(a) represents skematically the shape of a Pb precipitate at an asymmetrical 90° tilt boundary in Al. The Pb precipitate is single crystal, faceted with respect to one matrix grain but necessarily not faceted on the gross scale with respect to the other matrix grain [11, 12]. As a consequence there would be some mismatch at the boundary as depicted in Fig.3b, if the faceted and spherical cap portions were perfect in shape. However, evidently the correction of this mismatch can be accomplished by a very small number of Al atoms at the boundary, accomodating the situation.

The rest of Fig. 3 shows pairs of cuboctahedral sections joined at 90° symmetrical (Figs. 3c and d) and at 90° asymmetrical tilt boundaries (Figs. 3e and f). The symmetrical [110] tilt boundary is a mirror plane of the two matrix grains and, hence, of the two Xe grains of a precipitate at the boundary. It is readily possible, therefore, for the Al cavity which confines the Xe bicrystal to assume a perfectly faceted shape which is free of topological mismatch along the cavity edges at the boundary. Xe atoms in precipitates at such a boundary simply distribute themselves accordingly. Off the symmetrical boundary orientation, however, this structural simplification cannot be fully realized and a small amount of boundary mismatch is inevitable for perfectly faceted sections of the cuboctahedra, as is evident in Fig. 3f for a Xe precipitate straddling the assymmetrical boundary.

The Xe precipitates exist in the first place at 300 K because of the confining surface tensions of the Al cavities within which they reside. It has been estimated from Xe lattice parameters that the Xe in the solid state is stabilized at 300 K by an equilibrium pressure of the order of 1 GPa [1]. Not unexpectedly, the shape of individual Xe bicrystals is dictated largely by the {100} and {111} Al/Xe interfacial energies, which are probably nearly identical to the corresponding Al surface energies. That is, it is probably the boundary compatibility for Al cavity shapes, straddling a grain boundary, which largely determines the Xe bicrystal morphologies, coupled with the fact that a low energy Xe boundary replaces Al grain boundary for the Xe bicrystal case.

Unfortunately it has not been possible to determine from the high resolution images the grain boundary structure of any of the Xe bicrystals, possibly because the matrix

boundary segments for which imaging conditions should have been adequate for this task were not truly edge-on (for imaging, the specimen is tilted off the [110] zone axis nominally about 3°). Many of the asymmetrical boundary segments in particular clearly appeared to be significantly inclined away from the edge-on orientation as can be seen in Fig. 2; i.e., they are not pure tilt but rather exhibit a significant twist component. A portion of the boundary in the lower part of Fig. 2 appears to be so inclined. While there are a number of Xe precipiates which appear to be very near this boundary, only a small number of small precipitates are straddling it, in contrast to the large precipitates in the asymmetrical boundary in Fig. 4. Probably the situation in Fig. 2 stems from the more extensive topological mismatch which would result for Xe precipitates straddling such a mixed matrix boundary than a pure tilt boundary. The degree of mismatch will depend on the precipitate size. Perhaps above some critical precipitate size, the energy increase for accommodation of mismatch at the boundary will outweigh the energy decrease associated with replacement of matrix grain boundary by Xe boundary, causing such a precipitate to avoid contact with the boundary and remain single crystal. It is not known whether the inclination of this boundary away from pure tilt occurred during preparation of the mazed bicrstalline Al or as a consequence of subsequent high dose electron irradiation.

Influence of 1 MeV electron irradiation

Under the influence of damage produced continuously by the electron beam, the Xe precipitates do not exist at equilibrium with their environment. This is clearly demonstarted by the range of sizes and shapes of fluid Xe precipitates in Fig. 2. comparison of Figs. 2 and 4 further reveals a pronounced gradient of Xe nanoprecipitate sizes in the vicinity of the matrix grain boundary. This is more obvious in the larger electron irradiation dose case (Fig. 2), for which the estimated total electron-induced damage is of order 50 dpa (displacements per Al atom). In addition there appears to be a large density of very small precipitates along the boundary in Fig. 4 (less than 10 dpa) but in Fig. 2 only a few well formed precipitates along that portion of boundary which exhibits significant symmetrical tilt character. Also in Fig. 2, as mentioned in the previous section, the largely asymmetrical portion of the boundary deviates significantly from [110], which may be a consequence of the high dose irradiation.

The boundary within the precipitate on the asymmetrical matrix boundary (the enlarged view inset in Fig. 4) appears not to completely coincide with the orientation of Al matrix boundary. It is unclear how such a situation might occur if, in fact, it does.

However, the image of the portion of this Xe precipitate in region Al-2 is also somewhat anomolous, the spacing of one set of (111) appearing to vary periodically. Image simulations have not been performed for any of the bicrystal precipitates, in part because of indeterminant short range variations in imaging conditions, which clearly exist in this heavily irradiation-damaged material, both from ion implantation and subsequent electron irradiation. Previous simulations for imaging of Xe precipitates within an Al matrix, however, have verified that structural reliability of experimental images is usually high for the off-axial imaging technique employed here [8]. In addition there is a significant amount of precipitate overlap within the image of any given boundary. Only a limited amount of useable information has been acquired in these particular experiments due to the difficulties in achieving similar imaging conditions over a given bicrystalline area and maintaining those conditions for an extended time period. Consequently effects of 1 MeV electron irradiation over periods longer than a few tens of minutes have not been documented in this study.

Fig. 5 is a series of three images grabbed from video tape, which was made during electron irradiation, demonstrating the migration of a small Xe precipitate (arrowed in Fig. 5a), which is a common occurence for small precipitates under irradiation, and its subsequent absorption into the boundary. In Fig. 5c the crystalline order in the image of this particle appears to be breaking down shortly before the precipitate disappears (Fig.5d). A detailed analysis of the random walk migration process will be published elsewhere, based on the electron-stimulated displacement of Al atoms at the Xe/Al interface. Briefly, under 1 MeV electron irradiation, Al is readily displaced with sufficient momentum transfer to traverse the Xe precipitate (the bulk displacement cross-section for Al is ~60 barns under 1 MeV electron irradiation and that for Al at the interfaces must be considerably larger). Neither the 1 MeV electrons nor recoiling Al will displace Xe out of a precipitate. The analysis applied to these observations yields a diffusion coefficient D' for this Xe particle of order 5×10^{-3} nm^2 / dpa where

$$\Sigma (\Delta s_i)^2 = 4 D' \Delta\Phi .$$

$\Sigma (\Delta s_i)$ is the cumulative root mean square displacement and $\Delta\Phi$ is the associated dose increment. This value is smaller by a factor of about 6 than one obtained previously for a Xe precipitate composed of roughly two-thirds as many atoms.

Concluding remarks

This study has shown that Xe precipitates at 90° [110] tilt boundaries in mazed bicrstalline Al are bicrystals, thereby replacing a segment of matrix grain boundary

with Xe grain boundary. Thus the precipitate/matrix interface is well faceted. This is in contrast to the case of Pb precipitates in this same matrix material, which are single crystals with Pb/Al interface faceting generally with respect to one of the Al grains only. Where the matrix boundary is inclined away from [110] and thus possesses a twist component, the larger Xe precipitates avoid the boundary. These observations can be rationalized qualitatively on a simple geometrical model which emphasizes the degree of topological mismatch associated with perfect faceting in both matrix grains. For the case of symmetrical tilt boundaries, the Xe precipitate can assume a shape for which the mismatch is zero. For matrix boundaries with an asymmetrical component, such mismatch is evidently corrected in the vicinity of the boundary by the matrix, the increase in energy for such accommodation being less than the decrease in energy associated with the replacement of a segment of matrix tilt boundary by Xe tilt boundary. If, however, the boundary is not pure tilt but has a sufficient twist component, the effect of the accommodation energy increase may be larger than that of the boundary replacement energy decrease for Xe precipitates of some critical size. In this case such Xe precipitates would necessarily avoid the matrix boundary and remain single crystals. A proper analysis of this problem would also have to take into account the Xe/Al {100} and {111} interfacial energies as well as excess energies associated with facet intersections and apeces.

Acknowledgments

The authors are indebted especially to Bernard Kestel and Loren Funk at Argonne National Laboratory for specimen preparation and ion implantation and to Edward Ryan for assistance with figures. This work was performed under the Japan-USA Scientific Exchange Agreement and was supported at the respective laboratories of the authors by the US Department of Energy under Contract Nos. W-31-109-Eng-38 (ANL) and DE-AC03-76SF00098 (LBNL) and by the Science and Technology Agency of Japan.

References

1 Templier C (1991) Inert gas bubbles in metals. In: *Fundamental Aspects Of Inert Gases in Solids*, ed. Donnelly S E and Evans J H, pp. 117–132 (Plenum Press, New York).

2 Liu A S, and Birtcher R C (1989) Precipitation of Ar, Kr and Xe in Ni at room temperature. In: *Processing and Characterization of Materials Using Ion Beams* (MRS Symposium vol. 128), ed. Rehn L E, Greene J, and Smidt F A, pp. 303–308 (Materials Research Society, Pittsburgh).

3 Donnelly S E, Furuya K, Song M, Birtcher R C and Allen C W (1997) 1 MeV electron irradiation of solid Xe nanoclusters in Al: an in-situ HRTEM study. In: *Proceedings of International Centennial Symposium on the Electron*, Cambridge, UK. In Press.

4 Mitsuishi K, Song M, Furuya K, Birtcher R C, Allen C W and Donnelly S E (1998) In-situ observation of atomic processes in Xe nanocrystals embedded in Al. In: *Atomistic Mechanisms in Beam Synthesis and Irradiation of Materials* (MRS Symposium vol. 504), ed. Barbour J C, Ila D, Roorda S and Tsugioka M, pp. (Materials Research Society, Pittsburgh). In Press.

5 Ishikawa N, Awaji M, Furuya K, Birtcher R C and Allen C W (1997) HRTEM analysis of solid precipitates in Xe-implanted aluminum. Nucl. Instr. Meth. Phys. Res B **127/128**, 123–126.

6 Ziegler J F, Biersack P J, and Littmark U (1985) *The Stopping and Range of Ions in Solids*, ed. Ziegler J F (Pergamon Press, New York).

7 Furuya K, Song M, Mitsuishi K, Birtcher R C, Allen C W and Donnelly S E (1997) Direct imaging of atomic structure of Xe nanocrystals embredded in Al. In: *Proceedings of International Centennial Symposium on the Electron*, Cambridge, UK. In Press.

8 Furuya K, Ishikawa N and Allen C W (1998) In-situ determination of shape and atomic structure of Xe nanocrystals embedded in aluminum. Submitted to: *J. of Micros.*

9 Dahmen U and Westmacott K H (1991) TEM characterization of grain boundaries in mazed bicrystal films of aluminum. In: *Structure/Property Relationships for Metal/Metal Interfaces* (Mat. Res. Soc. Symp. Proc. vol. **229**), ed. Romig A D, Fowker D E, and Bristowe P D, pp. 167–178 (Materials Research Society, Pittsburgh.)

10 Private communication.

11 Johnson E, Johansen A, Hinderberger S, Xiao S-Q, and Dahmen U (1996) Structure and morphology of nanosized lead inclusions in aluminum grain boundaries. *InterfaceSci.* **3**, 279–288.

12 Johnson E, Dahmen U, Xiao S-Q, and Johansen A (1996) Equilibrium shapes of Pb Inclusions at 90° tilt boundaries in Al. In: *Proc. 54th Ann. Mtg. Micros. Soc. of Amer.* ed. Bailey G W, Corbett J M, Dimlich R V W, Michael, J R, and Zaluzec N J, pp. 364–365 (San Francisco Press, Inc., San Francisco.)

Figure captions

Figure 1. Selected area electron diffraction pattern of a [110] zone-axis mazed Al bicrystalline material, showing the two crystal orientations rotated by 90°. One orientation has been marked with white dots. Orientations of symmetrical (S) and asymmetrical (A) boundary traces are also indicated.

Figure 2. General overview of portions of two Al grains (Al-1 and Al-2) and their associated grain boundary after electron irradiation damage of approximately 50 dpa (with respect to bulk Al). (100) facet orientations are indicated for both matrix grains, as well as the orientations of symmetrical (S) and asymmetrical (A) boundary traces. The asymmetrical boundary exhibits a significant twist component. The inset is an enlargement of the Xe precipitate indicated, straddling a matrix boundary of mixed character.

Figure 3. Drawings of idealized precipitates at symmetrical and asymmetrical 90° tilt boundaries. (a) and (b). Pb on a asymmetrical boundary viewed parallel to the boundary ([110]) and normal to the boundary ([100] in upper left grain). (c) and (d). Xe on a symmetrical boundary viewed parallel to the boundary ([110] in upper left grain) and in perspective nearly parallel to the boundary. (e) and (f). Xe on a asymmetrical boundary viewed parallel to the boundary ([110]) and normal to the boundary ([100] in upper left grain).

Figure 4. Portions of two Al grains (Al-1 and Al-2) and their associated grain boundary after electron irradiation damage of less than 10 dpa (with respect to bulk Al). (100) facet orientations are indicated for both matrix grains, as well as the orientations of symmetrical (S) and asymmetrical (A) boundary traces. The inset is an enlargement of the Xe precipitate indicated, straddling an asymmetrical matrix boundary.

Figure 5. A relatively large (5 nm diameter) Xe precipitate on a nearly symmetrical 90° tile boundary in Al and a small (1.7 nm diameter) Xe precipitate (a) initially near the boundary, (b) after 1m 47.4s, having moved one $(111)_{Al}$ lattice spacing, (c) after 1m 47.4s, possibly disordering as it is absorbed into the boundary or it coalesces with another Xe precipitate in the boundary and (d) after 1m 58.3s, completing coalescence.

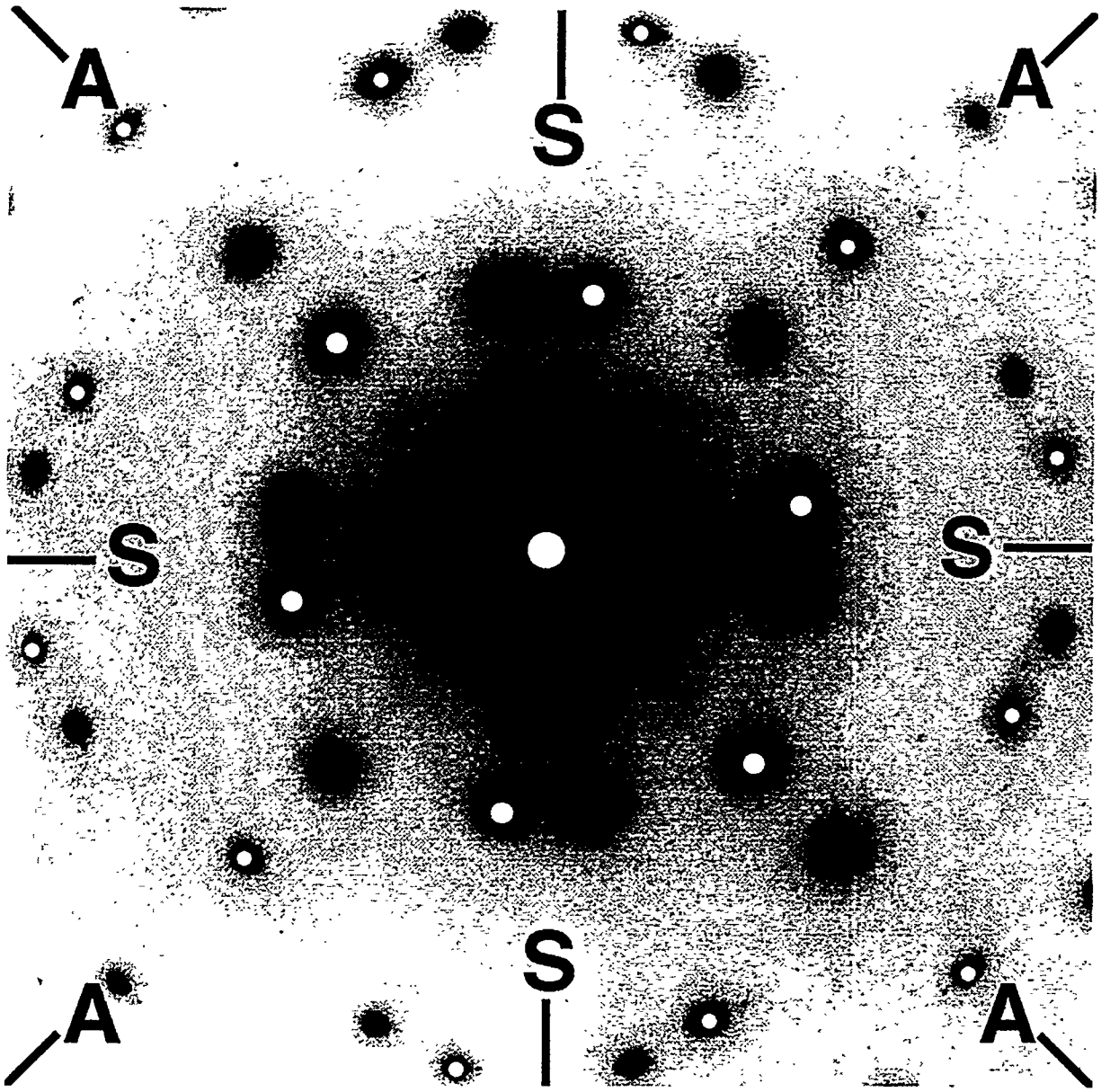

ALLEN FIG. 1

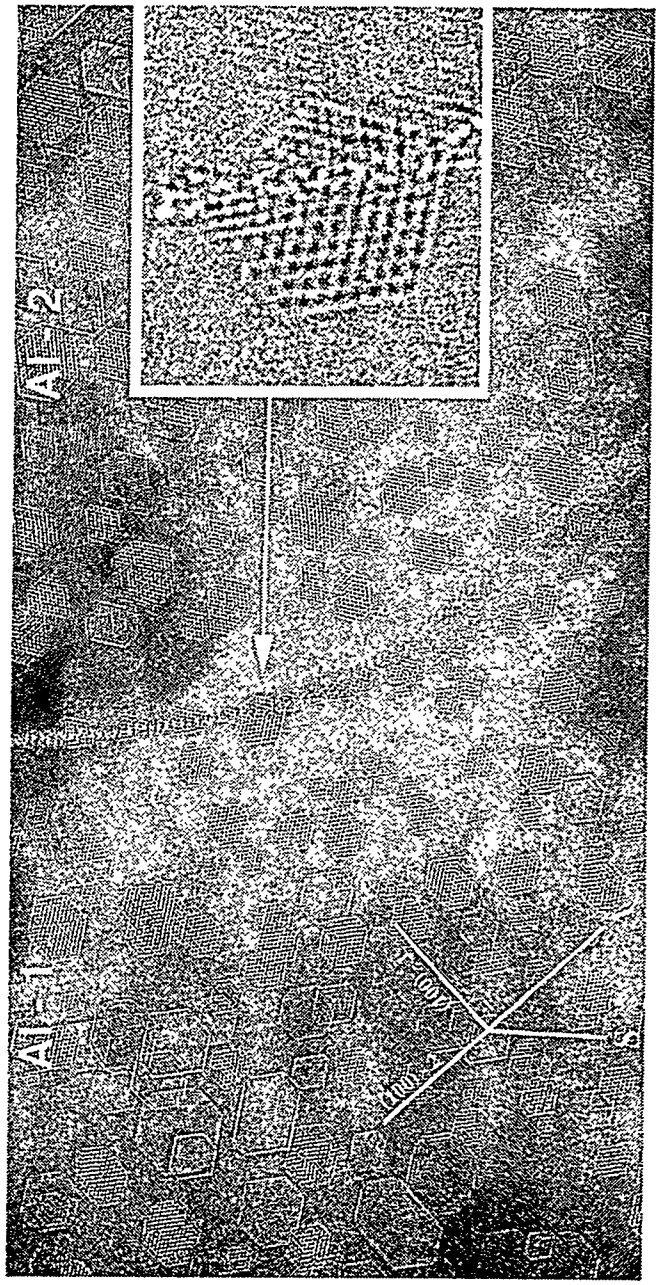
Al 2
Al 1

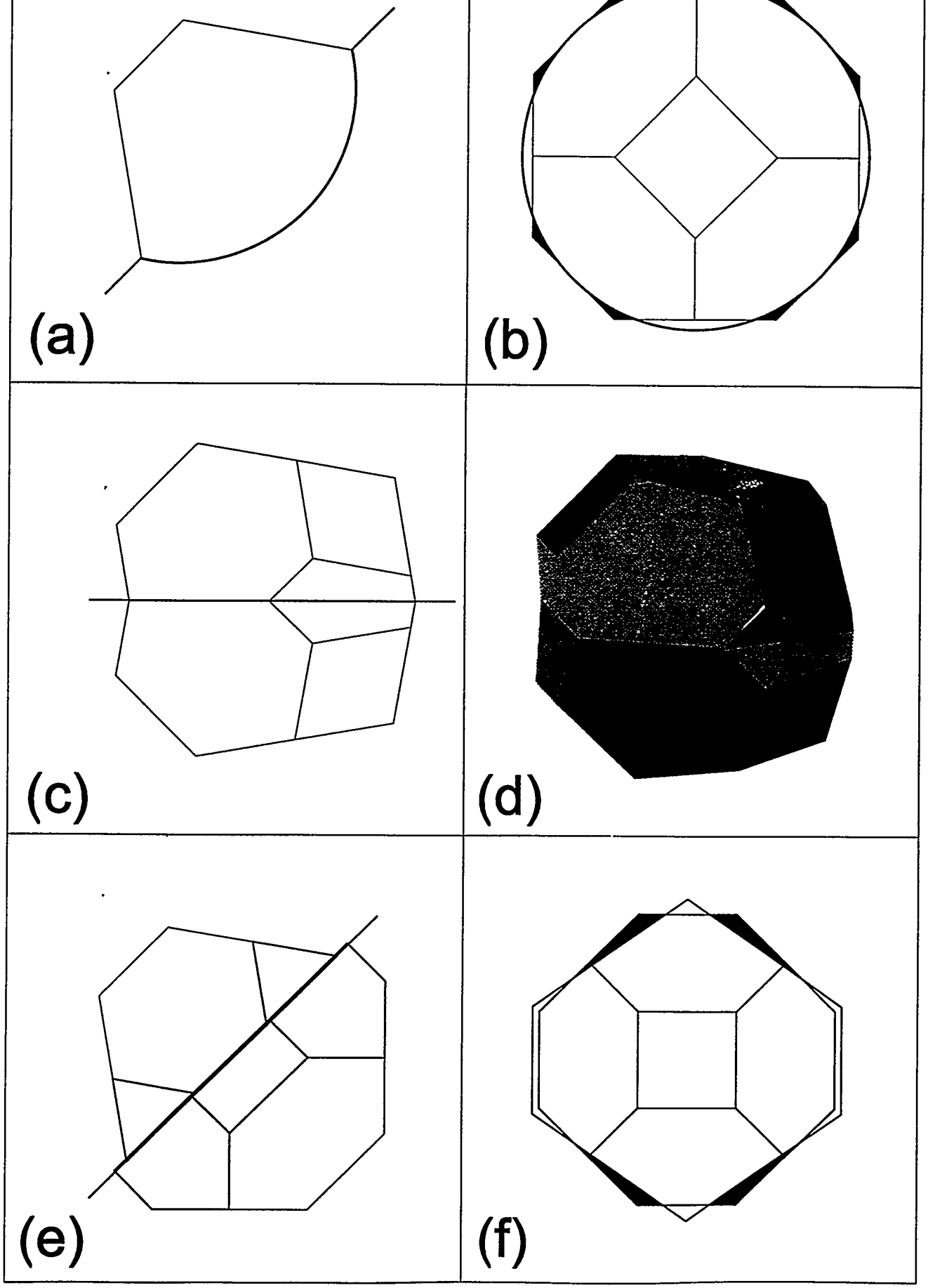
(a)
(b)
(c)
(d)
(e)
(f)

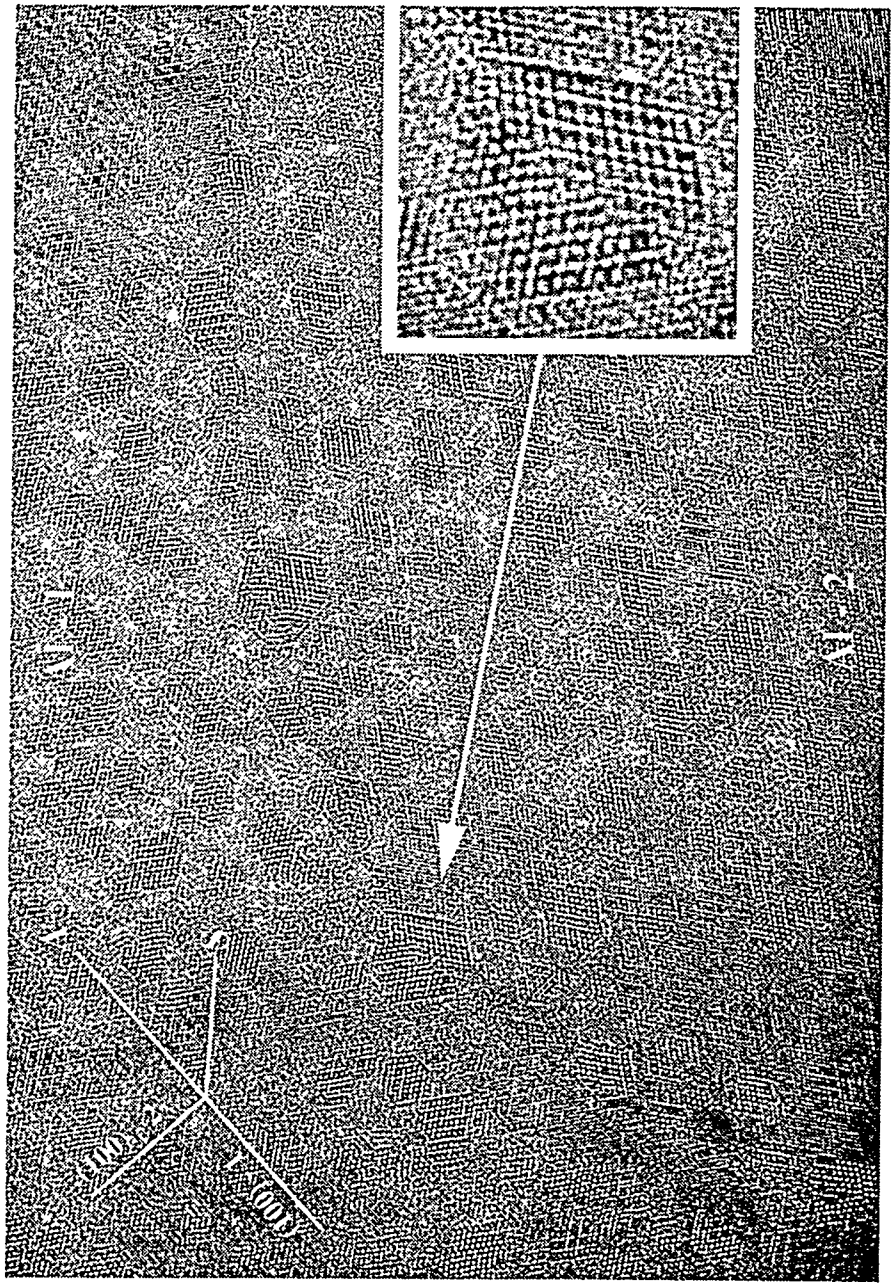
(100)
(001)

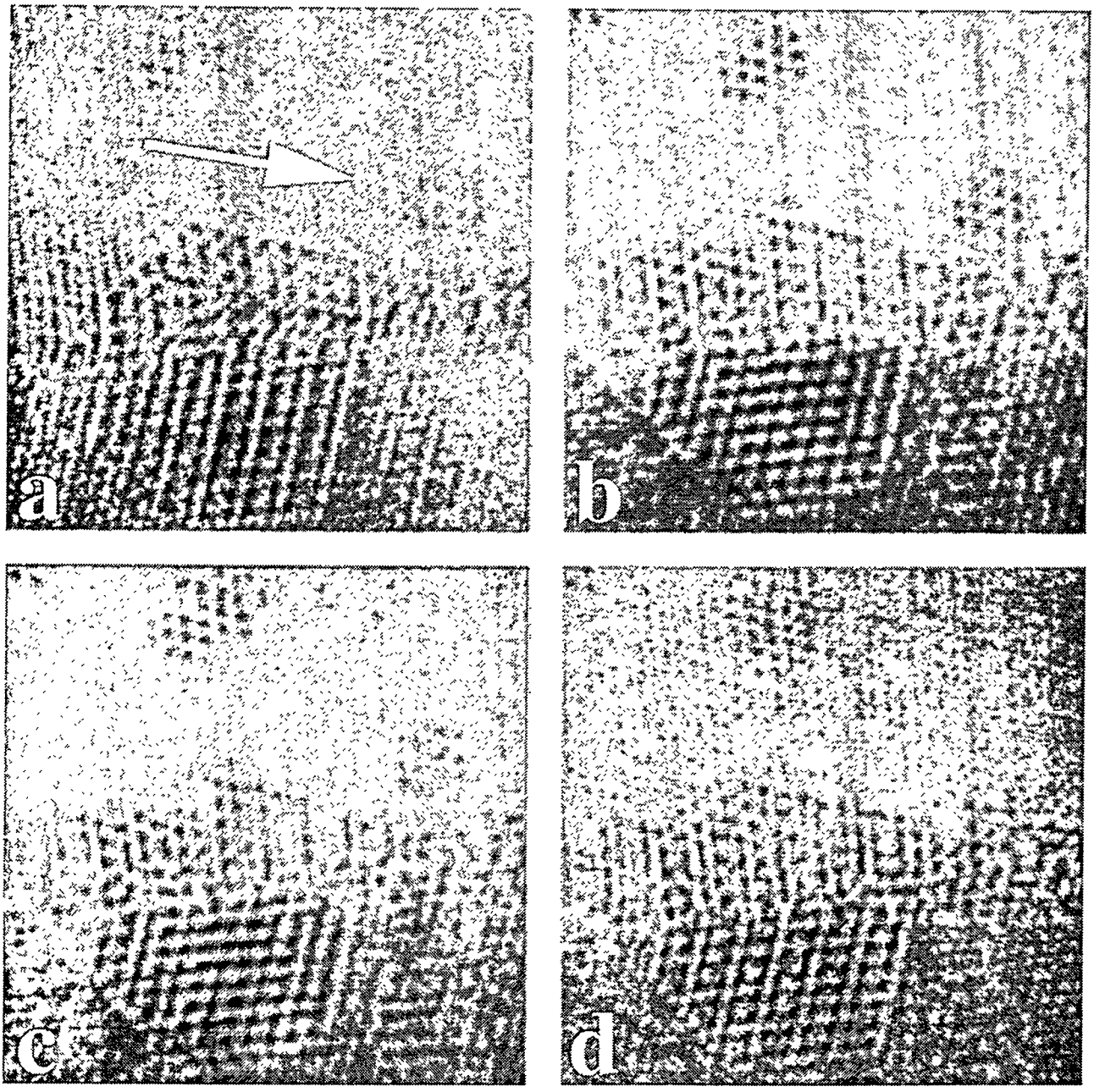
a
b
c
d